Article published online: 2024-05-13

The beauty of pediatric musculoskeletal ultrasound

Die Schönheit des pädiatrischen muskuloskelettalen Ultraschalls

Authors

Elena E Drakonaki[1, 2], Miraude Adriaensen[3], Paolo Simoni[4], Maria Pilar Aparisi Gomez[5, 6, 7]

Affiliations

1 Department of Anatomy, University of Crete School of Medicine, Heraklion, Greece
2 Department of MSK imaging, Diagnostic and Interventional Ultrasound Practice, Heraklion, Greece
3 Department of Medical Imaging, Zuyderland Medical Centre, Heerlen, Netherlands
4 Department of Rheumatology, Centre hospitalier universitaire de Liege, Liege, Belgium
5 Radiology, Auckland City Hospital, Auckland, New Zealand
6 Radiology, Instituto Musculoesquelético Europeo (IMSKE), Valencia, Spain
7 Department of Anatomy and Medical Imaging, Faculty of Medical and Health Sciences, University of Auckland, Auckland, New Zealand

Keywords

ultrasound, soft tissues, diagnostic radiology

received 12.1.2024
accepted after revision 26.3.2024
published online 13.5.2024

Bibliography

Rofo 2025; 197: 172–185
DOI 10.1055/a-2300-2821
ISSN 1438-9029
© 2024. Thieme. All rights reserved.
Georg Thieme Verlag KG, Oswald-Hesse-Straße 50, 70469 Stuttgart, Germany

Correspondence

Miraude Adriaensen, MD, PhD, MSc, EDiMSK
Department of Medical Imaging, Zuyderland Medical Centre, Henri Dunantstraat 5, 6419PC Heerlen, Netherlands
miraude@gmail.com

ABSTRACT

Purpose Ultrasound is a powerful technique in pediatric imaging and musculoskeletal (MSK) imaging in many specific clinical scenarios. This article will feature some common and less common spot diagnoses in pediatric musculoskeletal ultrasound.

Materials and methods Cases were collected by members of the Educational Committee of the ESSR (European Society of musculoSkeletal Radiology) and the Pediatric Subcommittee of the ESSR with expertise in musculoskeletal ultrasound.

Results Fifteen clinical entities are discussed based on the features that allow diagnosis by ultrasound.

Conclusion Clinical history, location, and ultrasound appearance are the keys to spot diagnoses when performing pediatric musculoskeletal ultrasound.

Key Points

- Ultrasound in pediatric musculoskeletal imaging can achieve a diagnosis in specific clinical settings.
- Clinical history, location, and ultrasound appearance are keys to spot diagnoses.
- Knowledge of spot diagnoses in pediatric musculoskeletal ultrasound facilitates daily clinical practice.

Citation Format

- Drakonaki EE, Adriaensen M, Simoni P et al. The beauty of pediatric musculoskeletal ultrasound. Rofo 2025; 197: 172–185

ZUSAMMENFASSUNG

Ziel Ultraschall ist in vielen spezifischen klinischen Szenarien eine leistungsstarke Technik in der pädiatrischen Bildgebung sowie in der muskuloskelettalen (MSK) Bildgebung. In diesem Artikel werden einige häufige und seltenere „Spot"-Diagnosen im pädiatrischen muskuloskelettalen Ultraschall vorgestellt.

Material und Methoden Die Fälle wurden von Mitgliedern des Bildungsausschusses der ESSR (European Society of musculoSkeletal Radiology) und des pädiatrischen Unterausschusses der ESSR mit Expertise im muskuloskelettalen Ultraschall zusammengestellt.

Ergebnisse Fünfzehn klinische Entitäten werden anhand der Merkmale, die eine Ultraschalldiagnose ermöglichen, erörtert.

Schlussfolgerung Klinische Anamnese, Lokalisation und Ultraschallbild sind die Schlüssel für „Spot"-Diagnosen beim pädiatrischen muskuloskelettalen Ultraschall.

Kernaussagen

- Der pädiatrische muskuloskelettale Ultraschall kann in bestimmten klinischen Situationen eine Diagnose stellen.
- Klinische Anamnese, Lokalisation und Ultraschallbild sind entscheidend für die Diagnosestellung.
- Die Kenntnis von „Spot"-Diagnosen im pädiatrischen muskuloskelettalen Ultraschall erleichtert die tägliche klinische Praxis.

This document was downloaded for personal use only. Unauthorized distribution is strictly prohibited.

Introduction

Ultrasound (US) is a useful technique in pediatric imaging and in musculoskeletal (MSK) imaging and it can be the primary diagnostic imaging modality in many specific clinical settings [1]. The advantages of US are well known and include no radiation, real-time static and dynamic multiplanar imaging, and relatively cheap, practical, and wide availability [2]. However, the main drawback of MSK US is a strong operator dependence with regard to technique as well as knowledge [1]. This article features some common and less common diagnoses in MSK US in the pediatric population.

Cases were collected and selected by members of the Educational Committee of the ESSR (European Society of musculoSkeletal Radiology) and the Pediatric Subcommittee of the ESSR with an expertise in MSK US. Fifteen cases are included.

In the first part, relevant US images are shown together with the relevant clinical information, the corresponding location of the human body, and the orientation of the US probe.

The second part will reveal the final diagnosis of each case followed by a short discussion. If available, another imaging correlate, i. e. photograph, conventional radiograph, or magnetic resonance (MR) image of the same patient is shown. At the end of the manuscript, a summary table is included matching the figure numbers with the corresponding diagnoses.

Therefore, the structure of the manuscript reflects clinical practice. Clinical information and US exam first will then lead to a diagnosis (i. e., a spot diagnosis if no other exams are needed in order to reach a final diagnosis). This manuscript may serve as a test for general radiologists of essentials in pediatric MSK US and additionally serve as an educational tool for beginners in pediatric MSK US.

Spot Diagnosis 1 (▶ **Fig. 1**)

A 3-week-old male baby presenting with swelling in the posterior aspect of the head and superior neck, and with a history of ventouse delivery, but otherwise well.

Ultrasound demonstrated a mildly complex collection underlying the scalp, posterior to the anterior fontanelle, overlying the parietal bone, and crossing the sagittal suture to extend over the right parietal bone. The collection was mildly compressible, and probe palpation generated discomfort. No underlying fracture was identified. In the context of history of ventouse delivery, findings were suggestive of a subgaleal hematoma.

A subgaleal hematoma is a potentially lethal condition in newborns (severe presentation occurring in 1.5/10,000 births) [3]. It is caused by the rupture of the emissary veins that connect the dural sinuses and the scalp veins. The blood accumulates between the epicranial aponeurosis of the scalp and the periosteum, typically crossing suture lines (this establishes the differential with a cephalohematoma). The virtual space is large, extending to the orbital margin anteriorly, the nuchal ridge posteriorly and to the temporal fascia laterally, and may hold a large amount of blood, resulting in hypovolemia [4]. In some cases, blood loss may be massive before hypovolemia shows.

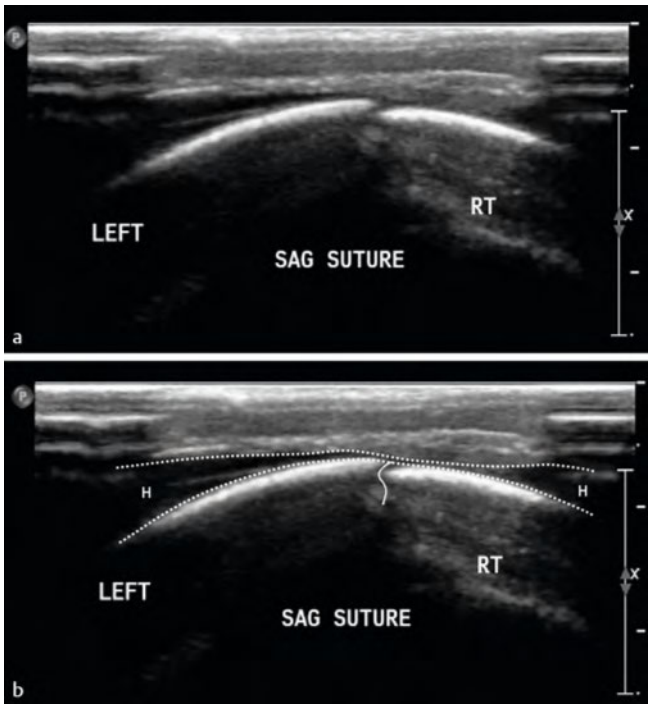

▶ **Fig. 1** 3-week-old male baby presenting with swelling in posterior aspect of the head and superior neck, and a history of ventouse delivery. **a** Transverse ultrasound image over the left parietal bone, sagittal suture, and right parietal bone. **b** Corresponding image with drawings. H = hematoma, LT = left, RT = right, SAG = sagittal suture.

The association with ventouse extraction is as high as 89 % [5], mainly related to inappropriate placement, but may also occur spontaneously.

Typical presentation is scalp swelling, which may fluctuate, an increased head circumference, and eventually hypotonia or tachycardia. Early diagnosis, careful monitoring, and prompt treatment are paramount for a good outcome.

On ultrasound, there is typically a collection underlying the scalp, with variable echogenicity, that may liquefy with time, and crosses sutures – not surrounded by the periosteum.

When subgaleal hemorrhage is suspected, hemoglobin measurement as well as coagulation studies should be performed. In the event of a difficult vacuum extraction, close observation during 8 hours of vital signs should be performed regardless of Apgar scores or need for resuscitation and close examination of the head [3].

Spot Diagnosis 2 (▶ **Fig. 2**)

A 10-year-old male patient presenting with a four-week history of submandibular swelling which is non-tender, but progressively increasing in size, with the left being more evident than the right.

Ultrasound demonstrated bilateral mildly irregular-shaped fluid collections, which extended through a dehiscence in the mylohyoid muscles, from the sublingual space into the submandibular space. These collections were easily compressible, and demonstrated no associated vascularity. Both submandibular glands

This document was downloaded for personal use only. Unauthorized distribution is strictly prohibited.

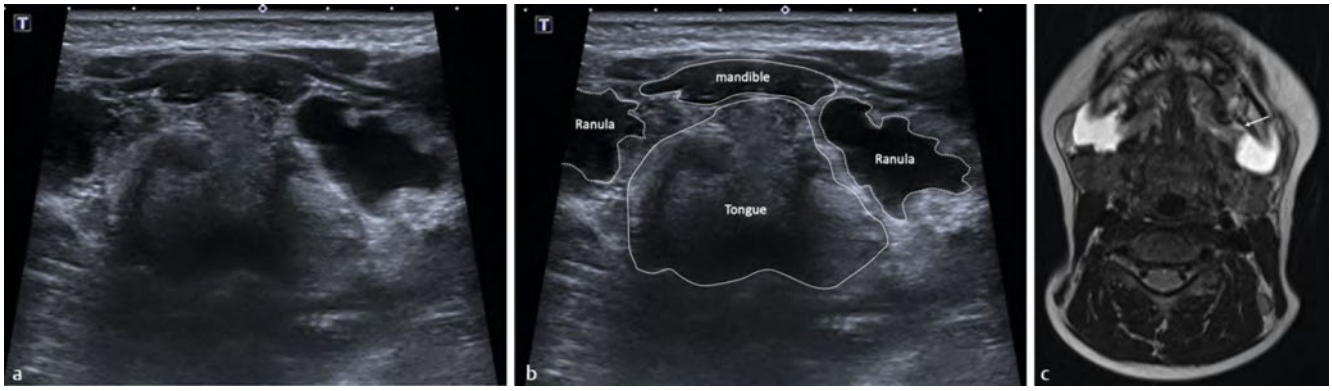

▶ **Fig. 2** 10-year-old male patient presenting with a four-week history of submandibular swelling which is non-tender, but progressively increasing in size, with the left being more evident than right. **a** Ultrasound, transverse plane through a submandibular approach demonstrating bilateral submandibular cystic spaces. **b** Corresponding images with drawings. **c** T2 in the axial plane demonstrating connection with the sublingual space lateral and posterior to the mylohyoid, with thin tail anterior to the submandibular gland visible on the left (arrow).

were mildly displaced, with normal echogenicity and configuration. Findings in the clinical context were suggestive of plunging ranulae. MRI performed for surgical planning confirmed the diagnosis.

Ranulae result from the obstruction of a sublingual gland, with formation of a mucous retention cyst. They may occur spontaneously or appear after trauma or surgery to the floor of the mouth. If small and limited to the sublingual space, they are considered simple. Plunging ranulae (or cervical ranulae) extend into the submandibular space from the sublingual space, dissecting along fascial planes, through a defect in the mylohyoid muscle or around the posterior/lateral aspect of it. It is common that ranulae have no proper lining (no epithelium) and represent pseudocysts surrounded by connective tissue [6].

Most ranulae contain normal saliva and are thin-walled with anechoic contents. However, if hemorrhage or infection occurs, the contents may be complex and the walls may be thick [6].

The main differentials are a thyroglossal duct cyst, usually seen in the midline (not lateral), a second branchial cleft cyst, which is usually located along the anterior border of the sternocleidomastoid muscle, and lymphatic malformations.

The key to diagnosis is to demonstrate the connection to the sublingual space, which may not be more than a small tail or neck. This is particularly important in plunging ranulae, which may be found some distance away from the sublingual space, and in which the neck or tail may have practically collapsed in the sublingual portion [6].

Ranulae may be treated with marsupialization, micro-marsupialization, CO2 laser, radiation, sclerotherapy, or surgical excision, which may be transoral or transcervical. The transoral approach allows for the complete removal of the sublingual gland, and is the option with no recurrence [7].

Spot Diagnosis 3 (▶ **Fig. 3**)

A 12-week-old male baby presenting with swelling on the right side of the neck, with no other clinical concerns. Ultrasound revealed the presence of fusiform enlargement of the mid-portion

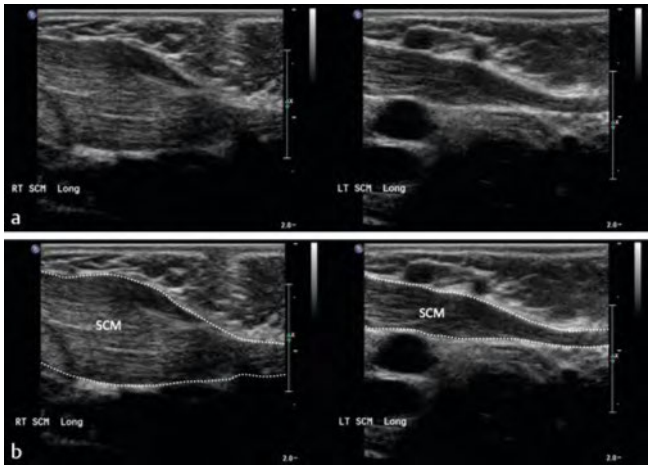

▶ **Fig. 3** 12-week-old male patient presenting with swelling on the right side of the neck. **a** Comparative longitudinal ultrasound images of the SCMs. **b** Corresponding images with drawings of the SCM. SCM = sternocleidomastoid muscle, RT = right, LT = left.

of the sternocleidomastoid (SCM) muscle on the right, with an otherwise normal fibrillar echotexture. The contralateral side was normal. There were no other pathological findings in the neck. The findings were typical for fibromatosis colli.

Fibromatosis colli is a benign, self-limiting condition that has a slight male predominance and normally involves the right SCM (approximately 3/4 of cases). It is thought to be related to birth trauma or intrauterine lie (breech), resulting in hemorrhage and subsequent fibrosis within the muscle belly [8].

Ultrasound appearance is diagnostic, with no further imaging workup required. The muscle belly is normally diffusely enlarged, with a fusiform shape and variable echogenicity – but no discrete mass – and shortened, with subsequent torticollis and deviation of the chin towards the contralateral side. Small foci of calcification may be apparent [9].

It is treated with physiotherapy and the condition usually resolves within a few months.

This document was downloaded for personal use only. Unauthorized distribution is strictly prohibited.

Spot Diagnosis 4 (▶ **Fig. 4**)

A 4-year-old girl accompanied by her parents presented at the emergency department reporting pain and mild swelling in the girl's right elbow following a sudden pull of her arm by her mother while walking to protect the girl from falling into a hole. Since the pull, the girl was unwilling to use the arm, constantly keeping the elbow slightly flexed and pronated. On physical examination, there was tenderness on the radial side of the elbow joint. Pulled elbow was suspected and so an X-ray was not ordered. Instead US scanning in the longitudinal plane over the anterior portion of the affected radio-capitellar joint with the elbow extended confirmed the suspected clinical diagnosis by showing an echogenic triangular soft tissue structure consistent with an enlarged synovial fringe interposed inside the radio-capitellar joint and mild thickening of the supinator muscle) due to edema. The corresponding image of the asymptomatic elbow was acquired for comparison, showing a normal supinator muscle and synovial fringe.

Pulled elbow (also known as nursemaid's elbow) is a subluxation of the radial head allowing it to slip under the annular ligament. It occurs in children younger than 5 years of age and is caused by a sudden longitudinal pull of the child's arm. It is a very common age-specific injury that has no clinical consequences following correct identification and reduction. As the diagnosis is based on the typical clinical history and findings, X-rays are not routinely required, and US imaging is used to confirm the diagnosis [10, 11]. One of the most reliable and reproducible US signs is the presence of synovial fringe enlargement (hook sign), suggesting soft tissue interposition in the joint [10, 11, 12], which disappears after successful reduction. Other signs include an entrapped and edematous supinator muscle, no visualization of the annular ligament (uncovered cartilage sign), and coronoid or olecranon fossa effusion [10]. As an enlarged synovial fringe may occasionally be found in the elbows of asymptomatic children with hyperlaxity, comparison with the non-injured side is necessary [12].

Spot diagnosis 5 (▶ **Fig. 5**)

A 13-year-old boy presented with symmetrical soft tissue thickening on the sides of the proximal interphalangeal (PIP) joints of the index, middle, and ring fingers bilaterally, which developed progressively, giving the fingers a fusiform appearance . No restriction of movement, skin changes, pain, or stiffness were present. US of the affected middle finger in longitudinal plane over the lateral side of the PIP joint showed thickening of the soft tissue (mainly the skin) of the affected finger compared to an unaffected finger. All other affected fingers showed the same ultrasound findings on the medial and lateral side of the PIP joints. No signs of PIP joint effusion or synovitis were seen. Coronal MR image showed high signal intensity in the soft tissue on the sides of the affected fingers with no signs of bone or joint involvement.

The clinical and imaging findings are typical of pachydermodactyly, which is a benign acquired form of digital fibromatosis, characterized by compact hyperkeratosis and thickening of the

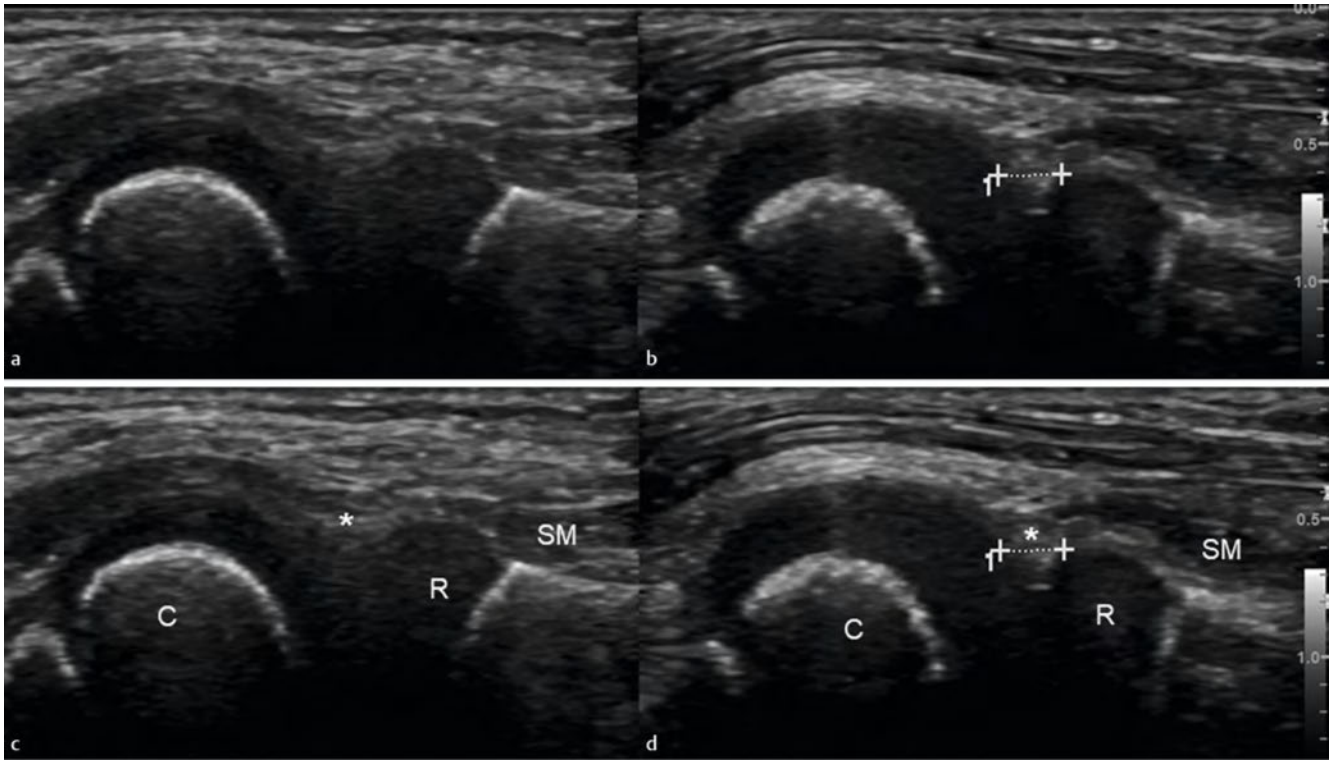

▶ **Fig. 4** US images of a 4-year-old girl with suspected pulled left elbow. Longitudinal US image of the extended left elbow over the radio-capitellar joint of the unaffected **a** and affected **b** side. Corresponding annotated images **c, d**. SM = supinator muscle, asterisk = synovial fridge, R = radial head, C = capitellum, callipers = radio-capitellar joint.

This document was downloaded for personal use only. Unauthorized distribution is strictly prohibited.

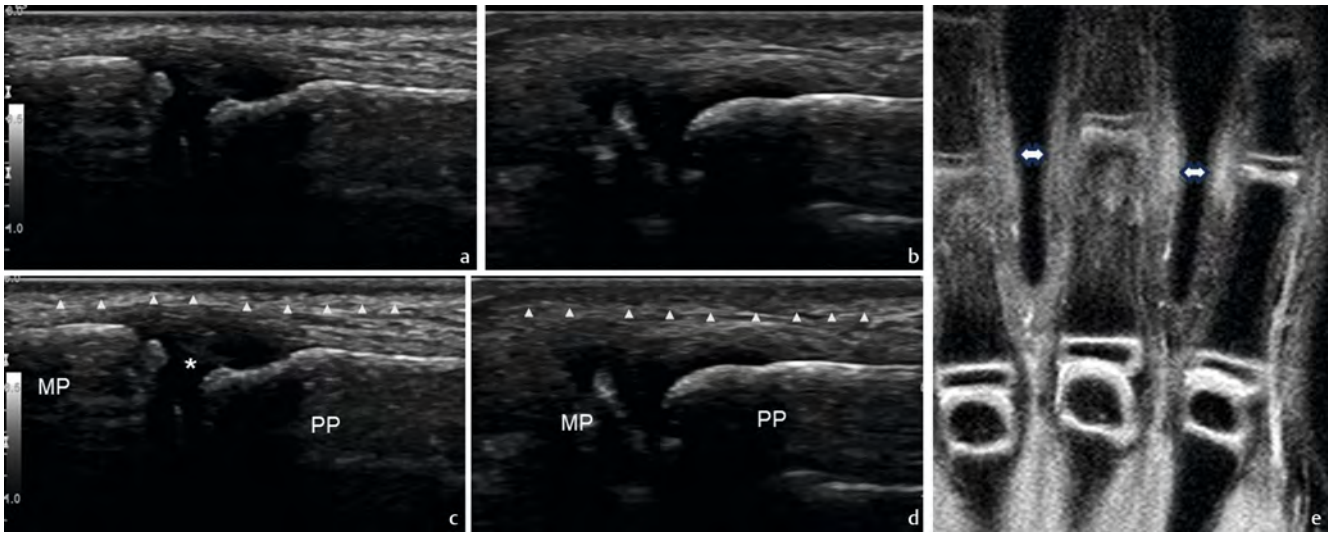

▶ **Fig. 5** 13-year-old boy with asymptomatic progressive symmetrical soft tissue thickening at the sides of the proximal interphalangeal (PIP) joints of the index, middle, and ring fingers. Longitudinal US images of lateral sides of an unaffected **a** and an affected **b** finger. Corresponding annotated US images **c, d**. The corresponding coronal STIR MR image **e**. MP = middle phalanx, PP = proximal phalanx, asterisk = PIP joint space, arrows = skin, double headed arrows = areas of soft tissue thickening and high signal intensity.

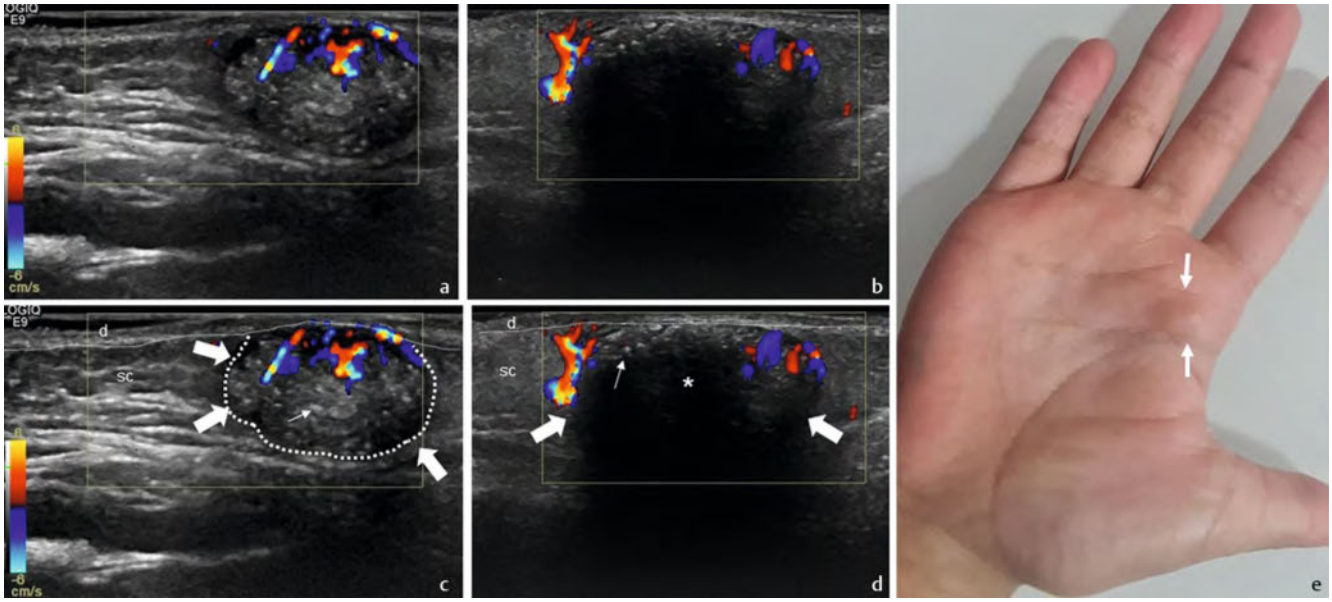

▶ **Fig. 6** A 5-year-old girl presented with a progressively growing hard lump on her palm. High-resolution (18Mhz) US scan of the lesion at presentation **a** and 8 months later **b**, corresponding annotated images **c, d**, as well as the clinical photo **e**. Thick dotted line = lesion, thin dotted lines = border between the dermis (d) and the subcutis (sc), thick arrows = hypoechoic rim, thin arrows = calcified foci, asterisk = posterior acoustic shadowing, arrow at e = lesion.

dermis typically affecting adolescent boys [13, 14]. Although of unknown etiology, an association with repetitive mechanical trauma or hormonal dysfunction has been reported [13, 14]. There are 5 different types, some including positive family history and association with tuberous sclerosis and Ehlers-Danlos syndrome [13]. The diagnosis is usually delayed or incorrectly considered as juvenile idiopathic arthritis. US can confirm the presence of skin involvement and exclude findings suggestive of arthritis, thus protecting the patient from unnecessary treatment.

Spot Diagnosis 6 (▶ Fig. 6)

A 5-year-old girl presented with a progressively growing hard lump on the palm of her hand. The child was otherwise asymptomatic with normal skin and no other symptoms.

US showed a heterogeneous, well-demarcated lesion located at the border between the dermis and the subcutis with an asymmetrical hypoechoic rim and echogenic foci of different sizes and shapes. There is Doppler signal indicating vascularity at the super-

This document was downloaded for personal use only. Unauthorized distribution is strictly prohibited.

ficial part of the lesion, mild acoustic attenuation at the deepest part, and no acoustic shadowing. A follow-up US scan 8 months later showed that the lesion retained the same US appearance only at its superficial parts, whereas the deeper part was obscured by posterior acoustic shadowing. The US characteristics, the age, and the natural history of the lesion are typical of a pilomatricoma. The lesion was excised and histology showed eosinophilic material with ghost cells, calcifications, granulation tissue, and inflammatory areas confirming the US diagnosis.

Pilomatricoma (also known as pilomatrixoma or calcifying epithelioma of Malherbe) is one of the most common benign skin lesions in childhood deriving from hair cortex cells and is characteristically located in the deep dermis or superficial subcutaneous layers of the skin. US shows different morphologic features depending on the stage of histologic evolution with early lesions including a hypoechoic heterogeneous echostructure with inner echogenic foci and a hypoechoic rim with posterior enhancement (early stage) or scattered dot calcifications or arc-like coarse calcifications with acoustic shadowing (late fully developed and regressive stages, respectively) [15]. In the very early phase, no obvious calcification and hypoechoic cystic formation may be encountered. Although very common in the pediatric age group, clinical detection is low, as it may clinically resemble a hemangioma or epidermoid cyst [15]. US may aid in the differential diagnosis by detecting the presence of calcifications, the hypoechoic rim and the characteristic evolution pattern on follow-up scans [15].

Spot Diagnosis 7 (▶ **Fig. 7**)

A 7-year-old boy presented with an asymmetric painless hard parasternal lump in the left thoracic wall. The parents recalled that it progressively appeared over the last year and was becoming more prominent. The boy was otherwise healthy and asymptomatic.

US of the anterior parasternal thoracic wall at the indicated area of the lump in comparison to the contralateral side at the same level showed asymmetry of the costal cartilage at the area just medial to the costochondral junction with anterior protrusion of the cartilage corresponding to the lump. No calcifications or tumor was seen. The normal anatomical layers of the anterior chest wall in the parasternal area were preserved (skin and subcutaneous fat, pectoralis muscle, cartilage and rib, pleura).

Palpable protrusions from the anterior chest wall of children may be alarming. However, silent asymmetries of the pediatric chest wall are very common pseudo-lesions, they are usually developmental rather than congenital, they become more prominent with growth, and they require no further imaging evaluation [16, 17]. As shown in CT studies, the most common variation is the prominent convexity of the costal cartilage (30.5 %), as in our case [16, 17]. US may be the first imaging modality to identify a conformational asymmetry associated with muscle, bone, or cartilage thus leading to diagnostic relief of parents while protecting children from an unnecessary radiation burden.

Spot diagnosis 8 (▶ **Fig. 8**)

A 4-month-old female baby presenting with a growing lump in the posterior aspect of the base of the neck/upper posterior chest.

Ultrasound examination revealed multiple serpiginous anechoic structures within a relatively echogenic region, which demonstrated color on Doppler examination.

Vascular tumors and malformations are a very large, heterogeneous group of lesions that may contain arterial, venous, or lymphatic vessels in a unique or combined way. The most common ones are soft tissue venous malformations and soft tissue hemangiomas. They are the most frequently diagnosed type of soft tissue tumor in the pediatric population.

The prevalence in neonates is 1–2 %, increasing to 12 % by 1 year of age [18].

Soft tissue hemangiomas may be found in the skin, subcutaneous tissue, skeletal muscle, and synovium and can be capillary, cavernous, arteriovenous, venous, and mixed.

Their appearance on ultrasound depends on the type. Generally, they appear as predominantly echogenic regions, which may contain cystic spaces (and mild posterior enhancement), dilated vessels (cavernous hemangiomas), and sometimes markedly echogenic foci, representing phleboliths. Spectral assessment may be variable.

In some cases flow may be almost undetectable, like in capillary hemangiomas, due to the small size of the vessels. The most common type that is typical in the pediatric population is the capillary hemangioma, which consists of small vessels tightly packed in connective tissue.

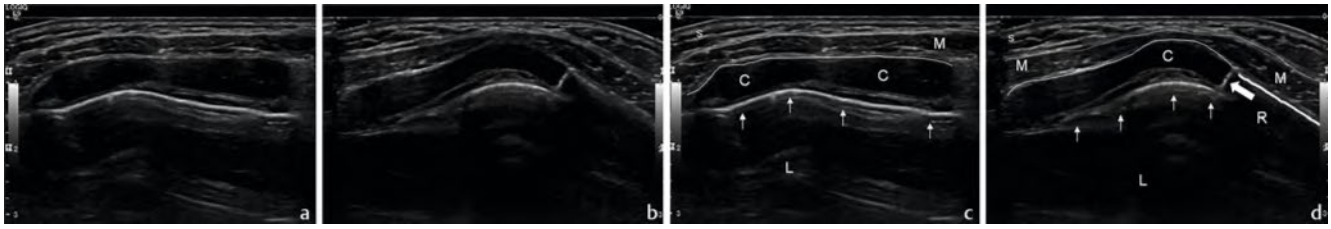

▶ **Fig. 7** A 7-year-old boy with left thoracic wall asymmetric parasternal painless lump. US image of the thoracic wall **b** in the area of the protrusion and along the long axis of the rib in the parasternal area and **a** on the contralateral side at the same level along the axis of the respective rib and corresponding annotated images **d, c.** S = skin and subcutaneous tissue, M = muscle, L = lung, C = costal cartilage, R = rib, thick arrow = costochondral junction, thin arrows = pleura, dotted line = border between subcutaneous layer and pectoralis major muscle. Thin line = border between pectoralis major muscle and costal cartilage. Thick line = border between pectoralis major muscle and rib.

This document was downloaded for personal use only. Unauthorized distribution is strictly prohibited.

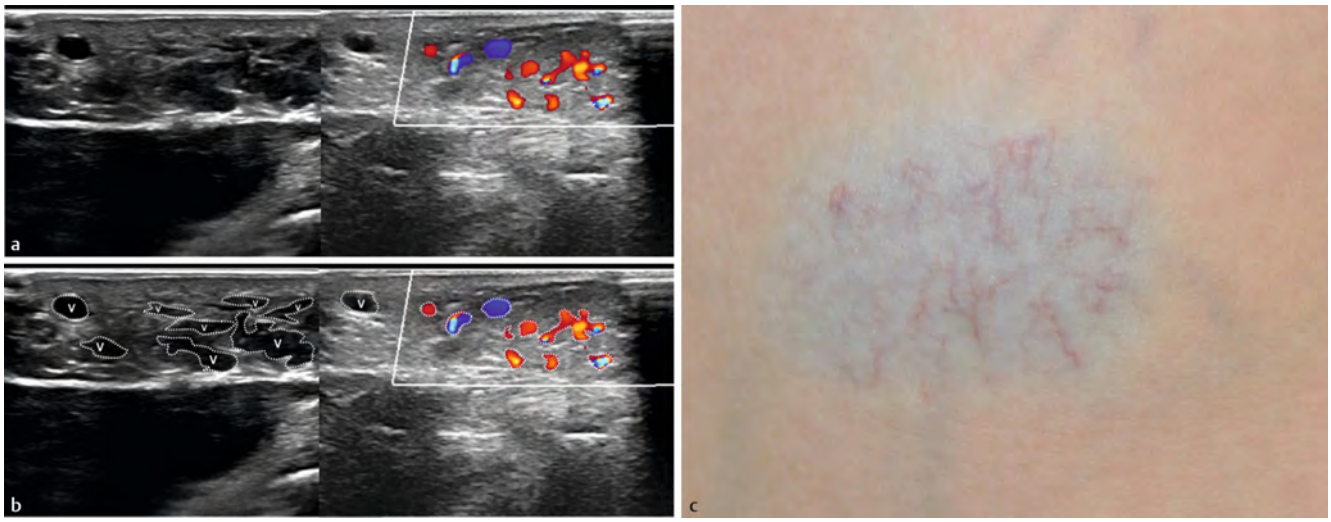

▶ **Fig. 8** 4-month-old female baby presenting with a growing mass in the posterior aspect of the base of the neck/upper posterior chest. **a** Longitudinal 2 D and Doppler ultrasound image over the region demonstrates multiple serpiginous anechoic structures within a relatively echogenic region that demonstrated color on Doppler interrogation. **b** Corresponding images with drawings. V = vessels. **c** The skin has bluish appearances and some superficial telangiectasias are evident.

▶ **Fig. 9** A 19-week-old fetus with a neural tube abnormality detected in the "skin line view" (sagittal spine view) on the second trimester anatomy scan. **a** "Skin line view" on19-week scan shows that the posterior ossification centers in the spine are absent in a segment from the level of L4 throughout the sacrum and there is a superficial soft tissue mass in the lumbosacral region, with heterogeneous, solid and mildly echogenic appearance. The skin line is seen to be continuous. Dedicated sagittal view on follow-up scan at 21w 5d shows the conus in detail, roots extending into the defect/soft tissue mass, and some tiny cystic spaces within the soft tissue mass. **b** Corresponding images with drawings. B = bladder, lmmc = lipomyelomeningocoele, V = vertebrae, c = conus. **c** Sagittal T2 from MRI performed at 33w 5d confirms the existence of a neural tube defect, with absence of the posterior arches in the midline and herniation of neural elements into the subcutaneous region. Distal nerve roots are tethered into the defect (zoomed in detail).

They normally appear shortly after birth and show a pattern of rapid growth over the first year of life, then become stable, and then start regressing as early as in the second year of life (reflected by decreased perfusion), normally disappearing before puberty. Treatment is usually not necessary but ultimately depends on location, growth, size, and complications, such as bleeding [19].

If located in the skin, they appear as blanching skin lesions with telangiectasias. Subcutaneous hemangiomas appear as bluish nodular lesions or plaques. On occasion, they may just present as palpable soft tissue masses.

Spot diagnosis 9 (▶ **Fig. 9**)

A 19-week-old fetus with a neural tube abnormality detected in the "skin line" view on the second trimester anatomy scan. The posterior ossification centers in the spine were absent from the level of L4 throughout the sacrum, and there was a superficial soft tissue mass in the lumbosacral region, with heterogeneous, solid appearances. The skin line was continuous. MRI performed at 33w 5d confirms the existence of a neural tube defect, with absence of the posterior arches and herniation of neural elements into the subcutaneous tissues. A layer of fat and skin covers the lesion, confirming this is a closed defect. The conus and distal nerve roots were seen to be tethered, extending down into to

This document was downloaded for personal use only. Unauthorized distribution is strictly prohibited.

the defect, with dilatation of the central canal inferiorly, at the level of the conus.

Neural tube defects occur when closure of the neural tube fails. This normally occurs when there is a failure in the secondary neurulation.

When this happens below the level of the cervical spine, defects are known as dysraphism or spina bifida. In spina bifida, there is defective fusion of the posterior vertebral arches. This has a spectrum, from a mere cleft with no herniation of the neurologic structures (spina bifida occulta) to exposure of neural structures through the defect in the posterior arch defect (spina bifida cystica).

The lumbosacral spine is the most common location, suggesting this region is more susceptible to genetic and/or environmental factors. Spina bifida is a relatively common occurrence among some populations, dependent on the geographic region (due to environmental factors) and genetics. Preventatively, fortified flour is supplemented with folic acid in some regions to avoid the condition [20].

Diagnosis is possible in utero, with the demonstration of the defects in the posterior arch and bulging in the posterior aspect in the "skin line" view (transverse spine in the lumbosacral level). Severe cases result in alterations in the morphology of the skull derived from the associated Arnold- Chiari type II syndrome that consists of a small biparietal diameter, ventriculomegaly, frontal bossing ("lemon" sign) elongation, and downward displacement of the cerebellum ("banana" sign), and a small or absent cisterna magna [21].

Lipomyelomeningoceles are in the spectrum of spina bifida and consist of complex anomalies in which there is a subcutaneous meningocele, fascial and bony defects, and a lipoma interfacing with the spinal cord, which may be located dorsally, dorsolaterally, or terminally. Externally, these lesions appear in the midline and can range from tiny inconspicuous fatty lumps to large masses that are usually accompanied by skin tags, portwine stains, and an altered intragluteal fold. Typically these fetuses/children do not have Chiari malformation, which gives them a better prognosis (no hydroencephaly) [22].

Many patients are asymptomatic and the natural history of these anomalies is unknown. However, progressive neurological deficits often occur because of spinal cord tethering or spinal cord compression as the fatty tissue enlarges [23].

Operative correction (careful microdissection with release of any tethering effect) in asymptomatic infants with a lipomyelomeningocele is controversial. The rationale for early operation in these patients is to release any tethering effect on the spinal cord to prevent neurologic (weakness, sensory loss), urologic (neurogenic bladder), or adverse orthopedic (scoliosis, leg-length discrepancies) consequences [24]. However, a significant number of patients have suffered the same deficits postoperatively that the surgery was planned to prevent. Some children progress despite surgery, which may be related more to a dysfunctional conus than to tethering effects. Recurrences are rare, but they do occur [25].

Spot Diagnosis 10 (▶ **Fig. 10**)

A 13-year-old boy presented with left hip pain and limping following a contact injury with a schoolmate during a soccer game.

US of the left hip/pelvis area showed an increased distance between the iliac bone (I) and the ossification center due to failure of the apophyseal cartilage (growth plate) and distal displacement of the secondary ossification center. The gap was filled with edema and hemorrhage. The direct tendon of the rectus femoris muscle is retracted distally and has a concave superior border due to a loss of tension. In comparison, the contralateral asymptomatic side retains a normal appearance of the enthesis chain. Corresponding coronal fluid-sensitive MR image of the pelvis confirms avulsion injury of the left anterior inferior iliac spine at the origin of the direct tendon of the rectus femoris with associated high signal intensity in the iliac bone and a speckle of bone with the retracted tendon and associated hematoma.

Apophyseal avulsion fractures of the rectus femoris tendon origin are common in children and adolescent football players. The direct tendon of the rectus femoris inserts at the secondary ossi-

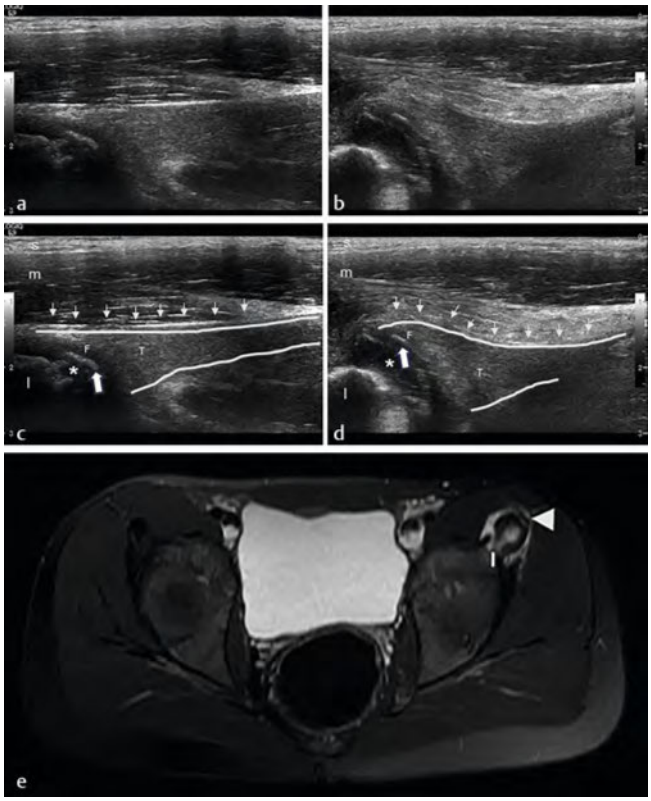

▶ **Fig. 10** A 13-year-old boy presented with left hip pain and limping following a contact injury with a schoolmate during a soccer game. US of the symptomatic area over the anterior inferior iliac spine on the longitudinal plane **b, d** in comparison to the contralateral asymptomatic side **a, c**. Corresponding axial fluid-sensitive MR image of the pelvis **e**. I = iliac bone (anterior inferior iliac spine), asterisk = apophyseal cartilage, thick arrow = ossification center, F = fibrocartilage between tendon enthesis and ossification center, T = direct tendon of the rectus femoris, m = iliopsoas muscle, s = skin, white lines = outline the direct tendon of the rectus femoris. Thick arrow head: apophysis.

This document was downloaded for personal use only. Unauthorized distribution is strictly prohibited.

fication center of the apophysis of the anterior inferior iliac spine with complete fusion occurring between 16–18 years of age [26, 27]. Since the growth plate is biomechanically weaker than the tendon, direct injury during adolescence results in avulsion displacement of the epiphysis rather than tendon rupture. As there are at least two more proximal tendons (indirect head and reflected head), the apophyseal displacement in the case of direct tendon avulsion is small and usually recovers well with conservative treatment with rest [28]. Operative treatment is reserved for widely displaced fractures (> 2 cm displacement) or when late complications such as heterotopic ossifications occur [28]. US allows imaging of the anatomy of the avulsion chain in detail due to high spatial resolution, thus allowing early diagnosis and recognition of the extent of apophyseal displacement [27].

Spot Diagnosis 11 (▶ **Fig. 11**)

A 10-month-old male infant presenting with fever for 24 hours, not weight-bearing on legs, and apparently sore during movement of the legs, particularly the left hip and knee.

Ultrasound examination revealed joint effusion with internal dependent debris. On the basis of the strong clinical suspicion of septic arthritis, aspiration was performed under ultrasound guidance. MRI was subsequently performed, which demonstrated surrounding myositis. The aspirate grew methicillin-resistant Staphylococcus Aureus. MRI was repeated several days later in order to rule out a collection because the patient was still spiking fevers despite adequate treatment. The MRI examination demonstrated no enhancement of the femoral epiphysis, typical of chondroepiphyseal involvement.

The most commonly involved joints are those in which blood flow in the metaphyses is abundant, such as the hip, shoulder, and knee.

Ultrasound is useful as the first tool of assessment in children (and in superficial joints in adults) and may demonstrate joint effusion with floating debris. However, please note this is not diagnostic. Effusion is a non-specific finding, common to several infectious and non-infectious hip pathologies. Doppler examination may show increased peri-synovial vascularity. However, the absence of increased vascularity does not rule out septic arthritis [29].

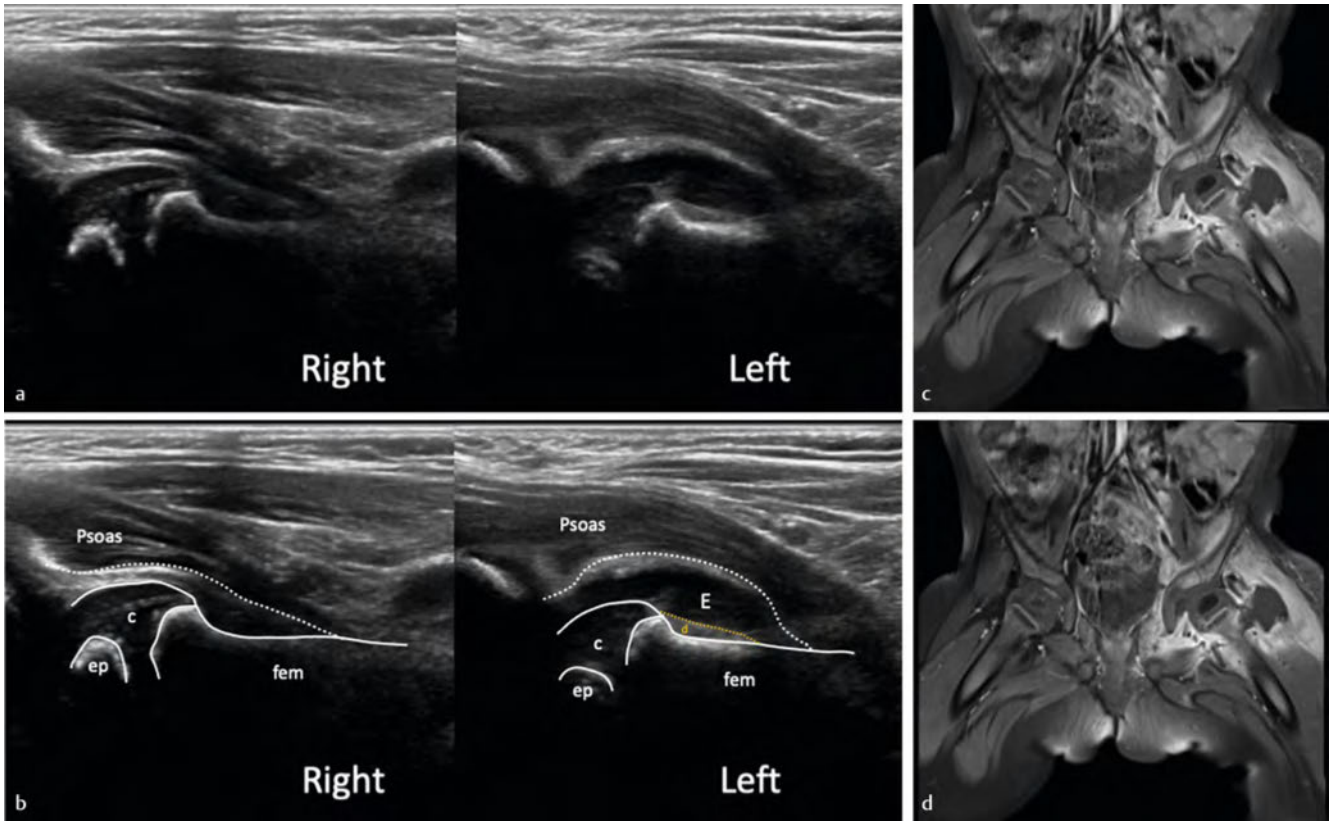

▶ **Fig. 11** 10-month-old male infant presenting with fever for 24 hours, not weight-bearing through legs, sore on movement of legs, particularly the left hip and knee. **a** Comparative longitudinal ultrasound examination reveals joint effusion on the left with internal dependent debris. The right hip is normal, with no effusion. Aspiration and lavage were performed. The aspirate grew methicillin-resistant Staphylococcus Aureus. **b** Corresponding images with drawings. E = effusion, d = debris, c = cartilage, ep = epiphyseal ossification center, fem = femur. **c** MRI (coronal T1 fat sat after intravenous gadolinium) performed on the same day demonstrates mild enhancement of the surrounding muscles. There is mild thickening and enhancement of the synovium. The joint was subsequently lavaged. **d** MRI was repeated some days later because the patient was still spiking fevers despite adequate treatment, to rule out a collection. Coronal T1 fat sat after intravenous gadolinium administration demonstrates no enhancement of the femoral epiphysis, typical of chondroepiphyseal involvement.

This document was downloaded for personal use only. Unauthorized distribution is strictly prohibited.

Clinical symptoms and laboratory tests can be helpful in differentiating transient synovitis from septic effusion and in selecting patients that require hip aspiration.

Kocher et al. [30] developed some criteria as a risk stratification score, to help with distinguishing septic arthritis from transient synovitis of the hip.

These are: (I) lack of weight bearing, (II) temperature of > 38.5° C, (III) C-reactive protein (CRP) > 2.0 mg/dL or erythrocyte sedimentation rate (ESR)> 40 mm/hr, (IV) white blood cells (WBC) > 12.0×10^9 cells/L.

The presence of fever ≥ 38.5 °, lack of weight bearing, ESR ≥ 40 mm/h, WBC > 12×10^9 cells/L has been associated with a predicted probability for septic arthritis of 99.6 % and 93 % [31]. CRP is the most significant predictor of septic arthritis. The association of CRP > 20 mg/L and a lack of weight bearing has a predictive probability for septic arthritis of 74 % [32].

On this basis, if 1 or 2 criteria are present (intermediate probability), an orthopedic/radiology review is warranted for consideration of aspiration. Ultrasound guidance can be used to guide aspiration.

If 3 or 4 criteria are present (high probability), the patient will often proceed straight to arthroscopic surgical drainage under orthopedics. In the high probability group, 48 % of patients have been found to have underlying osteomyelitis [33]. Ultrasound cannot rule out osteomyelitis and, therefore, MRI is indicated to rule out bone involvement. Osteomyelitis should be suspected if bone marrow edema extends into the medullary space in the setting of proven septic arthritis.

Children younger than the age of 30 months have an increased propensity for chondroepiphyseal infection. This may sometimes only be seen on gadolinium-enhanced T1 sequences and not on non-contrast T1 and fluid-sensitive sequences or with other techniques (bone scintigraphy). Active epiphyseal infection is seen as one or more areas of decreased or absent enhancement of the epiphyseal cartilage which normally enhances uniformly. The reason for this peculiar behavior on MRI remains controversial and may be related to direct infection or to ischemic phenomena.

Epiphyseal damage during infancy can result in growth disturbance and, therefore, gadolinium use in this age group is advised [34].

If not recognized and left untreated, septic arthritis may result in irreversible joint damage within 48 hours of the onset of infection. The white blood cells that enter the infected joint release proteolytic enzymes that cause extensive tissue damage. Osteonecrosis may also be a sequela of septic arthritis, due to compromised circulation.

Spot Diagnosis 12 (▶ **Fig. 12**)

An 11-year-old male patient presenting with a palpable mass on the medial side of the left distal upper leg. Ultrasound showed a bony exostosis in continuity with the distal femur seen as a continuous echogenic line covered by a hypoechogenic cap with a maximum thickness of 1.5 millimeters in keeping with an osteochondroma (i. e., cartilaginous exostosis). No signs of an overlying mechanical bursitis were noted. In addition, an X-ray was performed confirming the ultrasound findings. An osteochondroma consists of a bony spur covered by a cap of hyaline cartilage [27]. Osteochondromas can be solitary or multiple (i. e., multiple hereditary exostosis syndrome) [27]. The distal femur, the proximal tibia, and the proximal femur are the most common locations of a solitary osteochondroma [27]. An osteochondroma can become symptomatic due to impingement on adjacent structures, the formation of a mechanical bursitis, or malignant degeneration (chondrosarcoma) [27]. The thickness of the cartilaginous cap can be measured by ultrasound and is related to the risk of malignant degeneration [27].

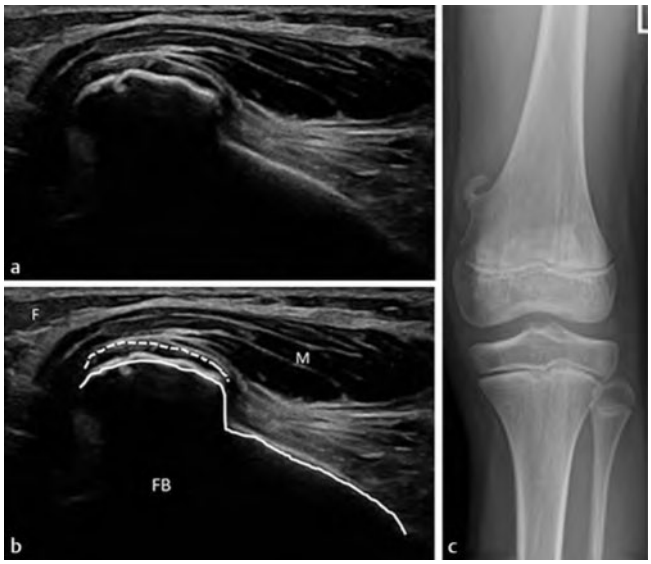

▶ **Fig. 12** 11-year-old male patient presenting with a palpable mass on the medial side of the left distal upper leg. **a** Longitudinal ultrasound image. **b** Corresponding image with drawing. F = fat, FB = femoral bone, M = muscle. **c** Conventional X-ray of the left knee in AP projection.

Spot diagnosis 13 (▶ **Fig. 13**)

A 13-month-old female infant presenting with recurrent episodes of a swollen left knee with recent reduced weight bearing and no fever. Her white blood cell count and inflammatory markers were elevated.

Ultrasound examination revealed hypoechoic, solid-looking material within the suprapatellar recess, extending down towards the joint. A small amount of this material was also present posteriorly in the popliteal region. On Doppler examination, there was relatively mild vascularity demonstrated within the synovium in the suprapatellar recess surrounding this material. The adjacent structures were normal. Findings were not typical for septic arthritis, and on that basis, MRI was performed. The examination showed marked enhancement of a thick synovium, with no enhancement of the intra-articular solid-looking component. Aspiration with culture and biopsy confirmed chronic synovial proliferation (pannus) and no infection.

Juvenile idiopathic arthritis (JIA) is a chronic autoimmune inflammatory disease and the most common rheumatic disease in

This document was downloaded for personal use only. Unauthorized distribution is strictly prohibited.

▶ **Fig. 13** 13-month-old female infant presenting with recurrent episodes of a swollen left knee with recent reduced weight bearing and no fever. The white cell count and inflammatory markers were elevated. **a** Longitudinal view over the suprapatellar recess demonstrates hypoechoic, solid-looking material distending the joint, and traces of effusion. **b** Corresponding image with drawings. Q = quadriceps, S = synovium, E = effusion, F = fat, c = cartilage, ep = epiphyseal ossification center. **c** Sagittal T1 fat sat and post-gadolinium demonstrates enhancement of a thickened synovium.

the pediatric population, with an estimated prevalence of 0.6 to 4 cases per 1,000 individuals [35].

The precise etiology of JIA is unknown, and infections, vaccinations, and trauma have been suggested in children with genetic susceptibility. JIA is an exclusion diagnosis that includes all

forms of childhood chronic arthritis of unknown cause. Inflammatory changes begin

before 16 years of age and persist for at least 6 weeks [36].

Based on the dominant clinical manifestations within the first 6 months of the disease as well as the results of laboratory tests, JIA is divided into subtypes: oligoarthritis, systemic arthritis, polyarthritis, psoriatic arthritis, enthesitis-related arthritis, and undifferentiated arthritis. Severe MSK disability affects 2 % to 5 % of children, and 31 % to 55 % of patients reach adulthood with active disease [37].

JIA is a clinical diagnosis, but imaging is a supporting tool and plays an important role in monitoring therapeutic response and detecting evolutive changes. Ultrasound (and

MRI) are increasingly used for evaluation, showing changes earlier than radiographs. Ultrasound is useful to confirm suspected clinical findings, assess the location and progression of JIA, to guide arthrocentesis and intra-articular therapy, and to follow up on the lesions during treatment.

Ultrasound can also detect associated tenosynovitis, bursitis, enthesitis, and panniculitis, and, in cases of progression, cartilage loss, cysts, and erosions.

In its pathophysiological course, the synovium is the first structure involved. Synovial hyperplasia followed by hypertrophy and hyperemia is observed in active disease. Inflamed synovium (pannus) is typically hypoechoic and concomitant to joint effusion. The pannus may eventually be misinterpreted as unossified cartilage or a soft tissue mass. Synovial hypertrophy may also show mixed or increased echogenicity, especially in chronic stages.

During follow-up, the synovium should be assessed in grayscale and Doppler, to detect active inflammation or fibrosis, in cases of successful treatment. US examination is more sensitive than clinical examination with respect to monitoring the efficacy of treatment, and information regarding disease activity is fundamental for the rheumatologist because residual (subclinical) activity is a proven risk factor for joint destruction [36].

Ultrasound has been proven to be as sensitive as MRI in identifying synovial effusion and pannus. Studies comparing both techniques showed a high level of agreement in the assessment of cartilage thickness [38].

Spot Diagnosis 14 (▶ **Fig. 14**)

A 12-year-old boy presented with a lump on the lateral side of the knee with associated mild knee pain. There were no sensory disturbances and range of motion was normal. US showed the presence of a multi-lobulated ganglion cyst anterolateral to the proximal tibia metaphysis deep to the muscles. The diagnosis of a juxta-articular ganglion cyst was confirmed on MRI which showed a cyst between the tibia and fibula and in close proximity to the tibiofibular joint.

Proximal tibiofibular joint ganglion cysts are mucin-filled synovial cysts originating from the proximal tibiofibular joint and extending inside the interosseous space, typically presenting with lateral knee pain and fullness. They are much rarer than wrist ganglia with only a few cases of tibiofibular ganglia reported in adolescent patients [39]. Due to their anatomical location, neurological symptoms secondary to compression of the common peroneal nerve are commonly encountered [39]. Ganglion cysts extending within the epineurium of an articular nerve branch of the peroneal nerve (intraneural ganglia) are even rarer in children [40]. US can show the cystic nature of the lesion, identify the common peroneal nerve, and look for signs of compression or intraneural extension [40]. MRI may better delineate the size and location of the cyst as well as the possible interosseous extension [39, 40].

Spot diagnosis 15 (▶ **Fig. 15**)

A 13-year-old male patient presenting with increasing lower leg pain just distal to the medial aspect of the knee, fever, and a lack

This document was downloaded for personal use only. Unauthorized distribution is strictly prohibited.

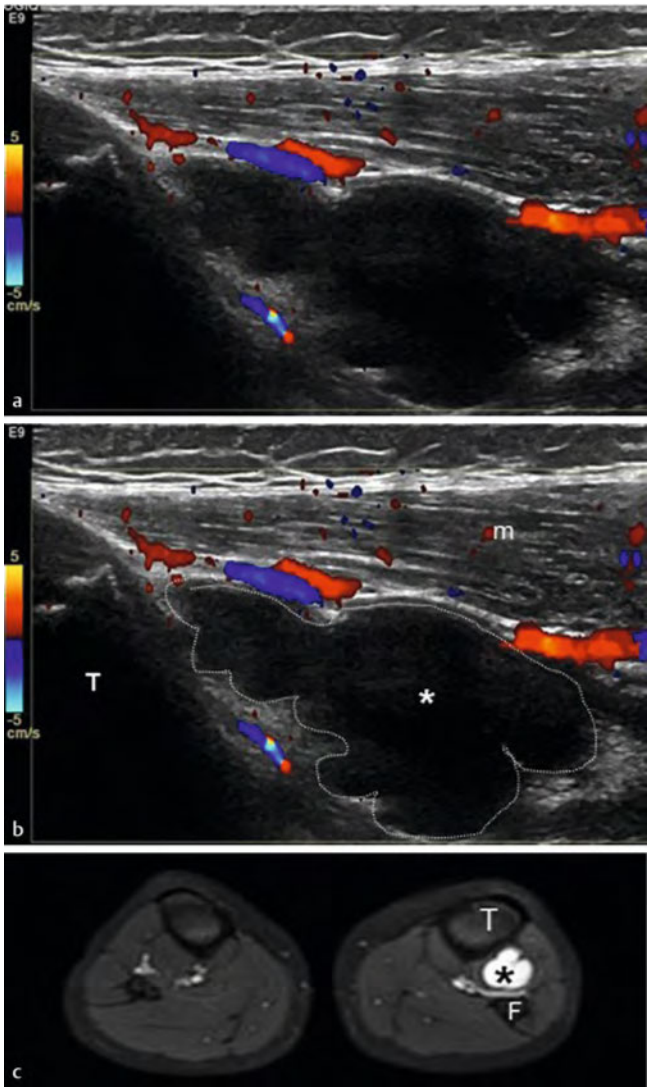

▶ **Fig. 14** A 12-year-old boy presented with a lump on the lateral side of the knee with associated mild knee pain and fullness but no sensory disturbances. US of the symptomatic area in longitudinal plane **a**. Corresponding image with drawings **b**. Corresponding axial fluid-sensitive MR image **c**. Asterisk = lesion, T = proximal tibia metaphysis, m = peroneus longus muscle F: fibula.

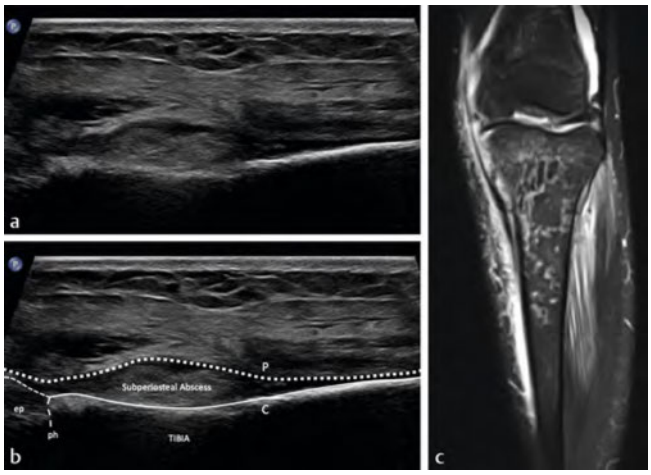

▶ **Fig. 15** A 13-year-old male patient presenting with increasing lower leg pain just distal to the medial aspect of the knee, febrile and not weight-bearing. **a** Ultrasound examination demonstrates subcutaneous edema and increased echogenicity of the subcutaneous fat in keeping with inflammatory change. Immediately superficial to the proximal tibial cortex, there is an ellipsoid echogenic structure with an overlying thin hypoechoic layer that did not compress with probe pressure. **b** Corresponding images with drawings. P = periosteum, C = cortex, ep = epiphysis, ph = physeal line. **c** Coronal T2 fat sat demonstrates extensive abnormal bone marrow signal of the proximal tibial epiphysis, metaphysis, and diaphysis, the subperiosteal collection in the medial proximal tibia and an additional small subperiosteal collection in the lateral proximal tibia. Note there is also joint effusion and an abnormal signal in the tibialis anterior and extensor digitorum longus muscle bellies, in keeping with myositis.

of weight bearing. On clinical examination, the anteromedial aspect of the left leg was swollen and tender.

Ultrasound examination demonstrated subcutaneous edema and increased echogenicity of the subcutaneous fat in keeping with inflammation. Immediately superficial to the proximal tibial cortex, there was an ellipsoid echogenic structure with an overlying thin layer of fluid that did not compress with probe pressure in keeping with a subperiosteal abscess of the tibia.

Acute hematogenous osteomyelitis (OM) is the most common form of osteoarticular infection in children, with the incidence peaking at around the age of 6. The clinical presentation is variable, combining pain, loss of function, fever, and sometimes general deterioration. Onset may be sudden and accompanied by a high fever [41]. Diagnosis is sometimes difficult due to a history of intercurrent trauma or antibiotics given for preceding infections. Osteomyelitis in children predominantly involves the metaphyses of long bones [41]. The lower extremities are affected in 70 % of cases [42]. From the metaphyseal focus, the infection can cause a subperiosteal collection.

The first radiographic sign of infection is soft tissue swelling, evident within 48 h of the onset of infection, and periosteal reaction, visible in 5–7 days. Osteolytic changes may take 7–10 days to 2 weeks to show on radiographs, but in one fifth of children radiographs remain normal after 2 weeks. Ultrasound is useful for the assessment of the soft tissues, is able to detect subperiosteal collection before radiographs, and is also useful to detect soft tissue collections. Besides, it is helpful to detect effusions that may be suggestive of joint involvement (in larger joints in which metaphyses are intraarticular). In newborns or younger toddlers, US can detect small infectious foci in the metaphysis or "metaphyseal-equivalent" regions and can guide aspiration of the effusion [43].

MRI is the gold standard in the evaluation of pediatric musculoskeletal infections and should be ideally performed within hours of the diagnosis of a suspected diagnosis of osteomyelitis.

Bone marrow signal intensity alterations on STIR images are visible 1 or 2 days after the onset of infection, while the OM focus is usually detected after 3–5 days. The typical MRI pattern includes low signal intensity on T1-weighted images, high signal intensity on T2-weighted and STIR images, and contrast enhancement of (subperiosteal) bone and/or soft tissues and abscess/collections. Sometimes the metaphyses have a physiological hy-

This document was downloaded for personal use only. Unauthorized distribution is strictly prohibited.

▶ **Table 1** Summary table matching figures with the corresponding diagnoses.

Figure	Spot diagnosis
1	Subgaleal hematoma
2	Plunging ranula
3	Fibromatosis colli
4	Pulled elbow
5	Pachydermodactyly
6	Pilomatricoma
7	Palpable costochondral pseudolesion
8	Hemangioma
9	Lipomeningocele
10	Apophyseal avulsion of the direct head of the rectus femoris tendon origin
11	Septic arthritis of the hip
12	Osteochondroma
13	Juvenile idiopathic arthritis (JIA)
14	Proximal tibiofibular joint ganglion cyst
15	Subperiosteal abscess of the tibia

perintensity on STIR images and a comparative image can be helpful in the early stages. Studies suggest contrast does not appear to improve the sensitivity or specificity for the diagnosis of osteomyelitis overall, and that if the fluid-sensitive images (*e.g.*, STIR, T2-FS) are normal, it may be omitted, as it provides no additional diagnostic value. However, contrast remains the reference standard to identify complications of osteomyelitis, such as intraosseous abscesses and chondroepiphyseal injury [44].

Conclusion

In this article we presented some common and less common diagnoses in pediatric MSK US (▶ **Table 1**). Clinical history, location, and US appearance are keys to spot diagnoses when performing pediatric MSK US.

Conflict of Interest

The authors declare that they have no conflict of interest.

References

[1] Martinoli C. Musculoskeletal ultrasound: technical guidelines. Insights Imaging 2010; 1 (3): 99–141. doi:10.1007/s13244-010-0032-9

[2] Drakonaki EE, Martinoli C, Vanhoenacker FM et al. The Beauty of Musculoskeletal Ultrasound: Spot Diagnoses. Fortschr Röntgenstr 2023; 195 (5): 385–392. doi:10.1055/a-1965-9961

[3] Davis DJ. Neonatal subgaleal hemorrhage: diagnosis and management. CMAJ 2001; 164 (10): 1452–1453

[4] Chadwick LM, Pemberton PJ, Kurinczuk JJ. Neonatal subgaleal haematoma: associated risk factors, complications and outcome. J Paediatr Child Health 1996; 32 (3): 228–232. doi:10.1111/j.1440-1754.1996.tb01559.x

[5] Sharman AM, Kirmi O, Anslow P. Imaging of the skin, subcutis, and galea aponeurotica. Semin Ultrasound CT MR 2009; 30 (6): 452–464. doi:10.1053/j.sult.2009.08.001

[6] Jain P, Jain R, Morton RP et al. Plunging ranulas: high-resolution ultrasound for diagnosis and surgical management. Eur Radiol 2010; 20 (6): 1442–1449. doi:10.1007/s00330-009-1666-1

[7] Chung YS, Cho Y, Kim BH. Comparison of outcomes of treatment for ranula: a proportion meta-analysis. Br J Oral Maxillofac Surg 2019; 57 (7): 620–626. doi:10.1016/j.bjoms.2019.06.005

[8] Bansal AG, Oudsema R, Masseaux JA et al. US of Pediatric Superficial Masses of the Head and Neck. Radiographics 2018; 38 (4): 1239–1263. doi:10.1148/rg.2018170165

[9] Bedi DG, John SD, Swischuk LE. Fibromatosis colli of infancy: variability of sonographic appearance. J Clin Ultrasound 1998; 26 (7): 345–348. doi:10.1002/(sici)1097-0096(199809)26:7 < 345::aid-jcu3 > 3.0.co;2-9

[10] Lee YS, Sohn YD, Oh YT. New, specific ultrasonographic findings for the diagnosis of pulled elbow. Clin Exp Emerg Med 2014; 1 (2): 109–113. doi:10.15441/ceem.14.009

[11] Sohn Y, Lee Y, Oh Y et al. Sonographic Finding of a Pulled Elbow: The "Hook Sign. " Pediatric Emergency Care 2014; 30 (12): 919–921. doi:10.1097/PEC.0000000000000299

[12] Varga M, Papp S, Kassai T et al. Two- plane point of care ultrasonography helps in the differential diagnosis of pulled elbow. Injury 2021; 52: S21–24. doi:10.1016/j.injury.2020.02.032

[13] Gallardo-Villamil A, Cano-Aguilar LE, Pérez-Muñoz E et al. Pachydermodactyly: Soft Tissue Enlargement of the Fingers in a Teenager. Cureus [Internet]. 2023 Jul 15 [cited 2024 Jan 4]. https://www.cureus.com/articles/165476-pachydermodactyly-soft-tissue-enlargement-of-the-fingers-in-a-teenager

[14] Bento da Silva A, Lourenço MH, Gonçalves MJ et al. Arthritis or maybe not? Pachydermodactyly: the great mimicker of juvenile idiopathic arthritis. ARP Rheumatol 2023; 2 (1): 78–82. doi:10.1016/j.carrev.2022.11.008

[15] Li L, Xu J, Wang S et al. Ultra-High-Frequency Ultrasound in the Evaluation of Paediatric Pilomatricoma Based on the Histopathologic Classification. Front Med 2021; 8: 673861. doi:10.3389/fmed.2021.673861

[16] Bako D, Yapici Ö. Silent anatomic variations of the pediatric chest: They might not be congenital. European Journal of Radiology 2021; 142: 109888

[17] Donnelly LF, Taylor CN, Emery KH et al. Asymptomatic, palpable, anterior chest wall lesions in children: is cross-sectional imaging necessary? Radiology 1997; 202 (3): 829–831. doi:10.1148/radiology.202.3.9051041

[18] Dubois J, Patriquin HB, Garel L et al. Soft-tissue hemangiomas in infants and children: diagnosis using Doppler sonography. AJR Am J Roentgenol 1998; 171 (1): 247–252. doi:10.2214/ajr.171.1.9648798

[19] Aparisi Gómez MP, Errani C, Lalam R et al. The Role of Ultrasound in the Diagnosis of Soft Tissue Tumors. Semin Musculoskelet Radiol 2020; 24 (2): 135–155

[20] Jin J. Folic Acid Supplementation for Prevention of Neural Tube Defects. JAMA 2017; 317 (2): 222. doi:10.3390/nu5114760

[21] Aparisi Gómez MP, Watkin S, Perry D et al. Anatomical Considerations of Embryology and Development of the Musculoskeletal System: Basic Notions for Musculoskeletal Radiologists. Semin Musculoskelet Radiol 2021; 25 (1): 003–21

[22] Imbruglia L, Cacciatore A, Carrara S et al. Abnormal skull findings in neural tube defects. J Prenat Med 2009; 3 (3): 44–47

[23] Hornig GW, Greene C. NEUROSURGICAL CONDITIONS. In: Ashcraft's Pediatric Surgery Elsevier; 2010: 235–246. https://linkinghub.elsevier.com/retrieve/pii/B9781416061274000197

[24] Bulsara KR, Zomorodi AR, Villavicencio AT et al. Clinical outcome differences for lipomyelomeningoceles, intraspinal lipomas, and lipomas of the filum terminale. Neurosurg Rev 2001; 24 (4): 192–194. doi:10.1007/s101430100177

This document was downloaded for personal use only. Unauthorized distribution is strictly prohibited.

[25] Perera D, Craven CL, Thompson D. Lumbosacral lipoma in childhood, how strong is the evidence base? A systematic review. Childs Nerv Syst 2023. doi:10.1007/s00381-023-06203-9

[26] Moraux A, Balbi V, Cockenpot E et al. Sonographic Overview of Usual and Unusual Disorders of the Rectus Femoris Tendon Origins. J of Ultrasound Medicine 2018; 37 (6): 1543–1553. doi:10.1002/jum.14352

[27] Bianchi S, Martinoli C. Ultrasound of the Musculoskeletal System. New York, Boulder: Springer NetLibrary, Inc. [distributor]; 2008

[28] Weel H, Joosten AJP, van Bergen CJA. Apophyseal Avulsion of the Rectus Femoris Tendon Origin in Adolescent Soccer Players. Children (Basel) 2022; 9 (7): 1016. doi:10.3390/children9071016

[29] Kang YR, Koo J. Ultrasonography of the pediatric hip and spine. Ultrasonography 2017; 36 (3): 239–251. doi:10.14366/usg.16051

[30] Kocher MS, Zurakowski D, Kasser JR. Differentiating between septic arthritis and transient synovitis of the hip in children: an evidence-based clinical prediction algorithm. J Bone Joint Surg Am 1999; 81 (12): 1662–1670. doi:10.2106/00004623-199912000-00002

[31] Kocher MS, Mandiga R, Zurakowski D et al. Validation of a clinical prediction rule for the differentiation between septic arthritis and transient synovitis of the hip in children. J Bone Joint Surg Am 2004; 86 (8): 1629–1635

[32] Singhal R, Perry DC, Khan FN et al. The use of CRP within a clinical prediction algorithm for the differentiation of septic arthritis and transient synovitis in children. J Bone Joint Surg Br 2011; 93 (11): 1556–1561

[33] Nguyen A, Kan JH, Bisset G et al. Kocher Criteria Revisited in the Era of MRI: How Often Does the Kocher Criteria Identify Underlying Osteomyelitis? J Pediatr Orthop 2017; 37 (2): e114–119

[34] Habre C, Botti P, Laurent M et al. Benefits of diffusion-weighted imaging in pediatric acute osteoarticular infections. Pediatr Radiol 2022; 52 (6): 1086–1094. doi:10.1007/s00247-022-05329-3

[35] Ravelli A, Martini A. Juvenile idiopathic arthritis. Lancet 2007; 369 (9563): 767–778. doi:10.1016/S0140-6736(07)60363-8

[36] Pracoń G, Aparisi Gómez MP, Simoni P et al. Conventional Radiography and Ultrasound Imaging of Rheumatic Diseases Affecting the Pediatric Population. Semin Musculoskelet Radiol 2021; 25 (1): 68–81

[37] Sudoł-Szopińska I, Jans L, Jurik AG et al. Imaging Features of the Juvenile Inflammatory Arthropathies. Semin Musculoskelet Radiol 2018; 22 (2): 147–165. doi:10.1055/s-0038-1639468

[38] Brunner E, Ting T, Vega-Fernandez P. Musculoskeletal ultrasound in children: Current state and future directions. Eur J Rheumatol 2020; 7 (Suppl. 1): S28–37. doi:10.5152/eurjrheum.2019.19170

[39] Khalefa MA, Hussain S, Bache EC. Common Peroneal Nerve Compression Neuropathy Due to a Large Synovial Cyst From the Proximal Tibiofibular Joint in a Teenager. Cureus 2023; 15 (10): e46562

[40] Bucher F, Maerz V, Obed D et al. Intraneural Ganglion of the Peroneal Nerve-A Rare Cause of Pediatric Peroneal Nerve Palsy: A Case Report. European J Pediatr Surg Rep 2022; 10 (1): e33–36. doi:10.1055/s-0042-1742608

[41] Vial J, Chiavassa-Gandois H. Limb infections in children and adults. Diagn Interv Imaging 2012; 93 (6): 530–546. doi:10.1016/j.diii.2012.03.014

[42] Bartoloni A, Aparisi Gómez MP, Cirillo M et al. Imaging of the limping child. European Journal of Radiology 2018; 109: 155–170

[43] Mellado Santos JM. Diagnostic imaging of pediatric hematogenous osteomyelitis: lessons learned from a multi-modality approach. Eur Radiol 2006; 16 (9): 2109–2119. doi:10.1007/s00330-006-0187-4

[44] Averill LW, Hernandez A, Gonzalez L et al. Diagnosis of osteomyelitis in children: utility of fat-suppressed contrast-enhanced MRI. AJR Am J Roentgenol 2009; 192 (5): 1232–1238. doi:10.2214/AJR.07.3400

This document was downloaded for personal use only. Unauthorized distribution is strictly prohibited.